Chemical Engineering Journal 155 (2009) 800–809

Contents lists available at ScienceDirect

Chemical Engineering Journal

journal homepage: www.elsevier.com/locate/cej

Intensifying esterification reaction between lactic acid and ethanol by pervaporation dehydration using chitosan–TEOS hybrid membranes

Jing Ma [a,b], Minhua Zhang [b], Lianyu Lu [a], Xin Yin [a], Jing Chen [a], Zhongyi Jiang [a,*]

[a] Key Laboratory for Green Chemical Technology of Ministry of Education, School of Chemical Engineering and Technology, Tianjin University, Tianjin 300072, China
[b] Key Laboratory for Green Chemical Technology of Ministry of Education, R&D Center for Petrochemical Technology, Tianjin University, Tianjin 300072, China

ARTICLE INFO

Article history:
Received 20 May 2009
Received in revised form 17 July 2009
Accepted 24 July 2009

Keywords:
Pervaporation
Hybrid membrane
Intensification
Ethyl lactate
Esterification

ABSTRACT

Esterification assisted by pervaporation separation can enhance the yield of ester for thermodynamically or kinetically limited reaction via selective removal of water from the reaction mixture. In the present study, organic–inorganic hybrid membranes were prepared by in situ hydrolysis and condensation of tetraethoxysilane (TEOS) within chitosan (CS) aqueous solution for pervaporation-assisted esterification of lactic acid with ethanol, catalyzed by Amberlyst 15 ion-exchange resin. The composition and structural properties of CS–TEOS hybrid membranes were investigated by FT-IR, XRD, TGA and contact angle. The dehydration performances of hybrid membranes were evaluated by pervaporation of aqueous ethanol solution. Comparing with CS pristine membrane, CS–TEOS hybrid membranes exhibited remarkably enhancing pervaporation property. Pervaporation-assisted esterification results suggested that the incorporation of pervaporation process to preferentially remove water from the reaction mixture substantially enhanced the yield of ethyl lactate from 66 wt.% to 80 wt.%. The effects of membrane casting solution recipe, reaction temperature, initial molar ratio of ethanol to lactic acid and catalyst loading amount on the process performance have been examined in detail.

1. Introduction

Esterification reactions are typically reversible and equilibrium-limited processes with ester and water as products. Due to the low energy consumption and ability to separate azeotropic mixtures, pervaporation has been proven as a promising technique for the selective removal of water from the esterification reaction mixtures and thus achieving a higher yield of ester [1–4].

Usually, batch or semi-batch reactor has been employed to pervaporation-assisted esterification process, where the reaction takes place with a homogeneous or heterogeneous catalyst, followed by pervaporation dehydration step with a permselective membrane. Water molecules pass through the membrane whereas the impermeable components are refluxed to the reactor. Obviously, the catalyst activity and the membrane performance are closely related to the final yield of ester. Presently, there have been a number of investigations concerning R&D of hydrophilic membranes, which can be catalogued into inorganic, organic, and organic–inorganic hybrid membranes. Inorganic membranes, such as zeolite and silica membranes have already been used for pervaporation coupled reaction. Tanaka et al. [5], Iglesia et al. [6] and Nemec and Gemert [7] investigated the esterification of acetic acid with ethanol, catalyzed by an ion-exchange resin, using zeolite T membrane, mordenite as well as zeolite A membranes and silica-based ceramic membrane, respectively. Yeung et al. [8–11] studied the knoevenagel condensation reaction in different zeolite membranes microreactor. While these inorganic membranes showed high dehydration efficiency, their industrialization process may be slow-paced for the difficult large-scale preparation and high manufacturing cost. In comparison, organic membranes have attracted much more attention. Several kinds of commercial organic membranes including PERVAP® 2201 [12], PERVAP 1005 (GFT) [13], GFT-1005 [14] have been introduced to the pervaporation–esterification coupling process for the synthesis of methyl acetate, ethyl acetate, ethyl lactate and diethyl succinate. In addition, Liu et al. [3,15] used cross-linked poly (vinyl alcohol) membranes to investigate the coupling process of pervaporation and esterification between acetic acid and *n*-butanol catalyzed by $Zr(SO_4)_2{\cdot}4H_2O$. These highly hydrophilic membranes could perform in situ removal of water and higher conversions could be acquired. However, the inherent disadvantages in stabilities seriously limit the applications efficiency of organic membranes. Therefore, it is necessary to develop the membranes with high hydrophilicity, thermal stability, good mechanical strength and superior chemical resistance which could be utilized in some relative harsh operating conditions [16,17]. Organic–inorganic hybrid material may be the best choice for having both the functionality of organic moiety and the stability of inorganic moiety [18].

* Corresponding author. Tel.: +86 22 23500086; fax: +86 22 23500086.
E-mail address: zhyijiang@tju.edu.cn (Z. Jiang).

1385-8947/$ – see front matter © 2009 Elsevier B.V. All rights reserved.
doi:10.1016/j.cej.2009.07.044

Nomenclature

A	effective area of the membrane (m^2)
DS	degree of swelling (%)
F, P	weight fractions
J	permeation flux (g/(m^2 h))
m_c	mass of ethyl lactate calculated from the wholly conversion of lactic acid in feed (g)
m_e	mass of ethyl lactate obtained in experiment (g)
R	initial molar ratio of ethanol to lactic acid
W	mass of membranes or permeate (g)

Greek letters

α	separation factor
α_D	diffusion selectivity
α_S	solubility selectivity

Organic–inorganic hybrid materials are viewed as the next generation materials for many applications, including the separation of aqueous–organic [19], organic–organic [20] and gas [21] mixtures. However, organic–inorganic hybrid membranes have seldom been reported in pervaporation-assisted esterification process. Budd et al. [22] employed zeolite/polyelectrolyte (chitosan/poly(4-styrene sulfonate)) multilayer pervaporation membranes for enhanced the yield of ethyl lactate. Adoor et al. [23] prepared aluminum-rich zeolite beta incorporated sodium alginate pervaporation membranes. The aluminum-rich zeolite beta, with its hydrophilic nature as well as molecular sieving effect and the favorable interaction with hydrophilic NaAlg, was responsible for enhancing the pervaporation dehydration efficiency, which resulted in a considerable increase in ethyl acetate conversion.

Generally, organic–inorganic hybrid membranes are prepared by simply blending inorganic particles into polymer matrix. However, the filled inorganic particles often exhibit serious aggregation leading to the non-selective voids at the organic–inorganic interface. In comparison, in situ generation of inorganic nanoparticles within polymer matrix has been demonstrated as an effective substitution [24,25].

Homogeneous catalysts, such as H_2SO_4, HCl [26], *p*-toluensulphonic acid [27], are frequently employed to esterification process. However, these catalysts have been found to attack membranes as well as the devices and are difficult to be separated from the products. As a result, there is an increasing concern on heterogeneous catalysts, such as ion-exchange resin [28], zeolite [29], solid super acid [30]. Ion-exchange resin has displayed comprehensive superiority in many situations [31]. Amberlyst 15 ion-exchange resin possesses distinct advantages including environmental benign, nontoxic, long-term chemical and physical stable [32] and easily recyclable [33–35], which has been successfully explored as a powerful catalyst for esterification reaction.

Biodegradable ethyl lactate ($C_5H_{10}O_3$) can be used as green solvent, food additive, perfumery and flavor chemicals. During ethyl lactate synthesis using lactic acid ($C_3H_6O_3$) and ethanol (C_2H_5OH) as reactants, dehydration constitutes the most troublesome task because ethyl lactate is soluble in water. In addition, ethanol and water can form azeotropic mixture. To addressing this problem, in the present study, the pervaporation separation with chitosan (CS)–tetraethoxysilane (TEOS) organic–inorganic hybrid membranes prepared by in situ hydrolysis and condensation was applied to esterification reaction of lactic acid and ethanol, with Amberlyst 15 ion-exchange resin as heterogeneous catalyst. The investigation focused on the following two issues: (1) the dehydration properties of CS–TEOS membranes, which was evaluated by pervaporation separation of ethanol/water mixture; (2) the enhanced conversion of ethyl lactate owning to the incorporation of pervaporation process.

2. Experimental

2.1. Materials

CS (the degree of deacetylation was 90.2%) was received from Jinan Haidebei Marine Bioengineering Co. Ltd. (Jinan, China). TEOS was obtained from Tianjin Guangfu Fine Chemical Research Institute (Tianjin, China). Lactic acid (88 wt.% lactic acid–water solution), ethyl lactate and anhydrous ethanol were purchased from Tianjin Jiangtian Chemicals Ltd. (Tianjin, China). Amberlyst 15 catalyst was supplied by Nankai University Chemical Factory (Tianjin, China), and the properties of Amberlyst 15 were shown in Table 1. The catalyst was repeatedly washed with ethanol and water prior to use to remove impurities and dried at 353.15 K under vacuum until the mass remained unchanged.

2.2. Membrane preparation

CS was dissolved in 2 wt.% acetic acid solution and stirred at 80 °C for 1 h to obtain 2 wt.% CS solution. It was then filtered and a known amount of TEOS as well as 0.5 M HCl were added to the filtrate. Subsequently, the solution was stirred for 2 h at room temperature and the resulting homogeneous solution was cast onto an organic glass plate with the aid of a casting knife. The membranes were allowed to dry at room temperature for 2–3 days and the completely dried membranes were peeled off. The mass ratio of TEOS to CS was varied as 0, 3, 6, 10, 20 and 33%, and the resulting CS–TEOS hybrid membranes were designated as CS, CS–TEOS (03), CS–TEOS (06), CS–TEOS (10), CS–TEOS (20) and CS–TEOS (33). Finally, the membranes were annealed at 120 °C for 2 h. The thickness of CS–TEOS membranes was 45 ± 5 μm measured by spiral micrometer.

2.3. Membrane characterization

FT-IR was employed to assess the interaction properties among different chemical groups of the hybrid membranes. The FT-IR spectra were recorded on a Nicolet 560 instrument equipped with both horizontal attenuated total reflectance (HATR) accessories. 32 scans were accumulated with a resolution of 4 cm^{-1} for each spectrum.

Crystallinity of the membranes was determined using a Rigaku D/max 2500 v/pc X-ray diffractometer in the range of 5–45° at the speed of 8° min^{-1} (Cu Kα 40 kV/200 mA).

Thermogravimetric (TG) analysis was conducted with a TGA-50 (SHIMDZU) thermogravimetric analyzer at a heating rate of 10 °C/min under a nitrogen atmosphere to analysis the thermal stability of CS–TEOS membranes.

The static contact angles for methylene iodide on the surfaces of CS and CS–TEOS membranes were measured using a contact angle

Table 1
The physicochemical properties of catalyst Amberlyst 15.

Properties	Amberlyst 15
Structure	Macroreticular
Matrix	Styrene–divinylbenzene
Functional group	$—SO_3^-H^+$
Particle size (mm)	0.4–0.6
% Moisture	<1.6
Density (g/mL)	0.70
Surface area (m^2/g)	77
Pore diameter (nm)	56
Total exchange capacity (mmol H^+/g_{cat})	4.7
Maximum operating temperature (°C)	100

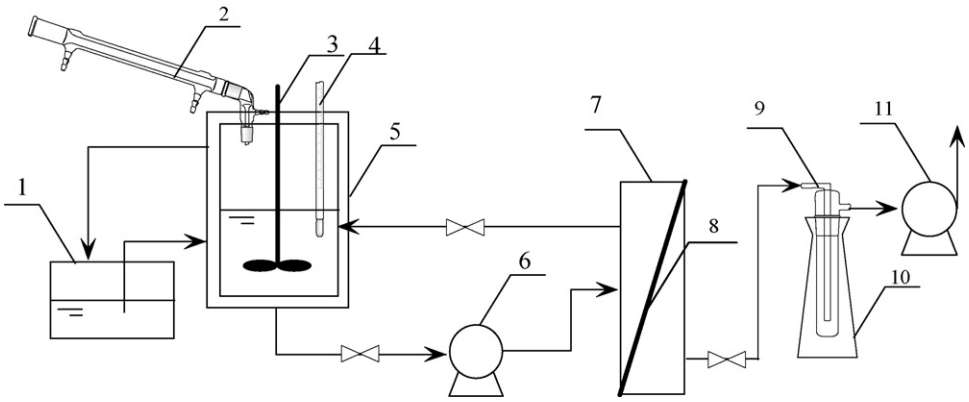

Fig. 1. Experimental apparatus for pervaporation-assisted esterification. (1) Heating bath, (2) condenser, (3) mixing blade, (4) thermometer, (5) esterification reactor, (6) feed pump, (7) membrane cell, (8) membrane, (9) permeate collection tube, (10) liquid nitrogen trap, and (11) vacuum pump.

goniometer (Erma Contact Angle Meter, Japan) at 25 °C. The drop of methylene iodide was introduced on the membrane using a micro syringe. All the membrane samples were stored in a vacuum oven at 25 °C before analysis.

2.4. Swelling measurements and sorption experiments

A piece of membrane sample (about 0.3 g) was dipped into 90 wt.% aqueous ethanol solution at 80 °C for 12 h to achieve equilibrium. Then, the membrane sample was taken out and wiped off the surface solution with tissue paper carefully, and weighed as quickly as possible. The liquid that was adsorbed in membrane was collected in a liquid nitrogen trap by desorbing the equilibrated sample in the purge-and-trap apparatus, and then analyzed by gas chromatography. The degree of swelling (*DS*) was calculated by Eq. (1):

$$DS(\%) = \frac{W_s - W_d}{W_d} \times 100 \quad (1)$$

The solubility selectivity α_S was calculated by Eq. (2) [36,37]:

$$\alpha_S = \frac{M_W/M_E}{F_W/F_E} \quad (2)$$

where W_s and W_d are the mass of the swollen and dry membranes respectively. M_W and M_E are the weight fractions of water and ethanol in the membrane respectively. F_W and F_E are the weight fractions of water and ethanol in the solution respectively.

According to the solution–diffusion model, diffusion selectivity (α_D) was calculated by Eq. (3):

$$\alpha_D = \frac{\alpha}{\alpha_S} \quad (3)$$

By considering the volatility of ethanol, all the sorption experiments were repeated at least three times, and the experiment errors were all within 5%.

2.5. Pervaporation experiments

Experimental apparatus for pervaporation dehydration experiments of ethanol/water mixture is presented in Fig. 1. The effective membrane area of P-28 membrane module (CM-Celfa AG Company, Switzerland) was 28.0 cm^2. On the permeate side, kept at low pressure (less than 1.0 kPa) with the help of a vacuum pump, permeate is condensed using a glass trap cooled with liquid nitrogen. The permeate flux was determined gravimetrically by weighing the mass of permeate collected. The performance of CS–TEOS membranes were usually expressed in terms of the permeation flux (J) and separation factor (α), which were calculated according to Eqs. (4) and (5):

$$J = \frac{W}{At} \quad (4)$$

$$\alpha = \frac{P_W/P_E}{F_W/F_E} \quad (5)$$

where W is the mass of permeate (g), A is the effective area of the membrane in contact with the feed (m^2), t is the permeation time (h), P_W and P_E are the weight fractions of water and ethanol in permeate, respectively, F_W and F_E are the weight fractions of water and ethanol in feed, respectively.

2.6. Pervaporation-assisted esterification experiments

The esterification reaction coupled with pervaporation was performed in a batch operation mode. Experimental equipment was the same as that originally described for pervaporation. Ethanol was added to the reactor together with Amberlyst 15 and heated to the reaction temperature. Lactate acid was heated to reaction temperature separately and then added to the reactor. Meanwhile, the reaction mixture was pumped continuously through the pervaporation unit with a feed rate of 60 L/h. This time was taken as the starting time for experiments. The reaction temperature was kept constant within ±0.5 °C by using water heating bath. The yield of ethyl lactate was calculated by Eq. (6)

$$\text{the yield of ethyl lactate}\,(\%) = \frac{m_e}{m_c} \times 100 \quad (6)$$

where m_e is the mass of ethyl lactate obtained in experiment and m_c is the mass of ethyl lactate calculated from the wholly conversion of lactic acid in feed.

2.7. Analytical procedures

About 1 mL reaction mixture was taken out at each sampling instant and immediately cooled in ice/water mixture to stop the reaction. Samples from both, the reactor and the permeate membrane side, were analyzed by gas chromatography using Agilent 4890, equipped with a thermal conductivity detector (TCD) and a column packed with GDX103 (Tianjin Chemical Reagent Co., China). The oven was operated at variable-programmed temperature, from 180 °C to 240 °C at a rate of 20 °C/min. The injector and detector were at 220 °C and 250 °C, respectively. Cyclohexanone was used as the internal standard.

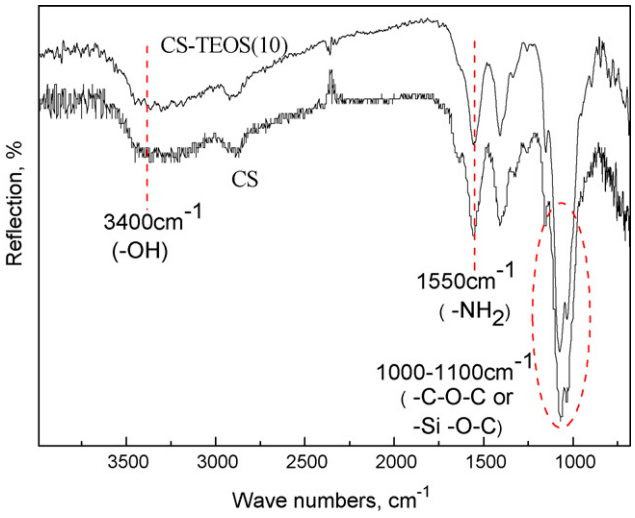

Fig. 2. FT-IR spectra of chitosan pristine membrane and CS–TEOS (10) hybrid membrane.

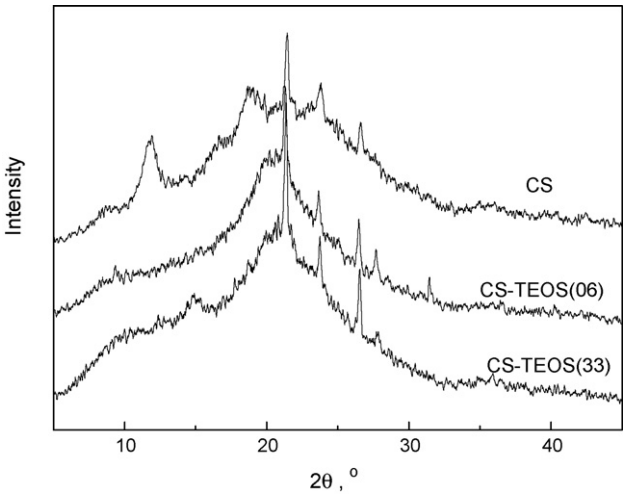

Fig. 3. XRD patterns of chitosan pristine membrane and CS–TEOS membranes.

3. Results and discussion

3.1. Membrane characterization

3.1.1. FT-IR

Fig. 2 showed the FT-IR spectra of CS pristine membrane and CS–TEOS (10) membrane. A characteristic strong and broad band at around 3400 cm^{-1} in CS pristine membrane spectra corresponded to —OH stretching vibrations. The intensity of this band decreased in CS–TEOS (10) membrane, which indicated that partial —OH groups of CS involved in condensation reaction with silanol groups of TEOS, forming covalently bonds between polymer segments. Furthermore, multiple bands in CS membrane spectra at around 1000–1100 cm^{-1} were assigned to —C—O—C stretching. The increase in the intensity of these bands for the CS–TEOS (10) membrane, suggesting the formation of —Si—O—C bonds [38], since Si—O stretching also appeared at the same wave numbers of C—O stretching. The characteristic peak at 1550 cm^{-1} was assigned as $—NH_2$ group [39], which apparently increased after incorporating TEOS. These observations indicated that the hydrogen-bonding interactions between amino groups and hydroxyl groups of CS chains weakened [40].

3.1.2. XRD

The membranes were also subjected to XRD analyses to evaluate the influence of inorganic fillers on crystalline structures of CS, and the results were presented in Fig. 3. As we know, CS usually exists in two crystal forms: form I has the major crystalline peaks at 11.2° and 18.0°, while form II has major crystalline peaks at 20.9° and 23.8° [40]. The introduction of TEOS dramatically interfered with the ordered packing of CS chains, resulting in the decrease of membrane crystallinity. The absence of the peak 11.2° suggested that a large number of hydrogen bonding formed in the CS chain was destroyed through cross-linking. The reducing crystallinity of CS membrane would decrease the compactness of polymer chain packing, which was advantageous to improve the water permeation.

3.1.3. TGA

The thermal stability and degradation behavior of the CS–TEOS membranes were evaluated by TGA under nitrogen atmosphere (Fig. 4(a)). The TGA curves displayed the first thermal event in the range 40–150 °C, which corresponded to a weight loss of approximately 15% and it was attributed to the evaporation of water loosely bound to the polymer. The second thermal event occurring in the range of 200–400 °C was attributed to further decomposition, to deacetylation and depolymerization of CS. The third event, for temperature higher than 400 °C, corresponded to the residual decomposition reactions [41]. This study only focused on the first stage of the thermal degradation occurring after the initial dehydration step, which occurred in the range 200–400 °C. The temperature corresponding to the maximum degradation rate, T_m, was gained from the DTG curves (Fig. 4(b)), which were 246 °C and 282 °C for

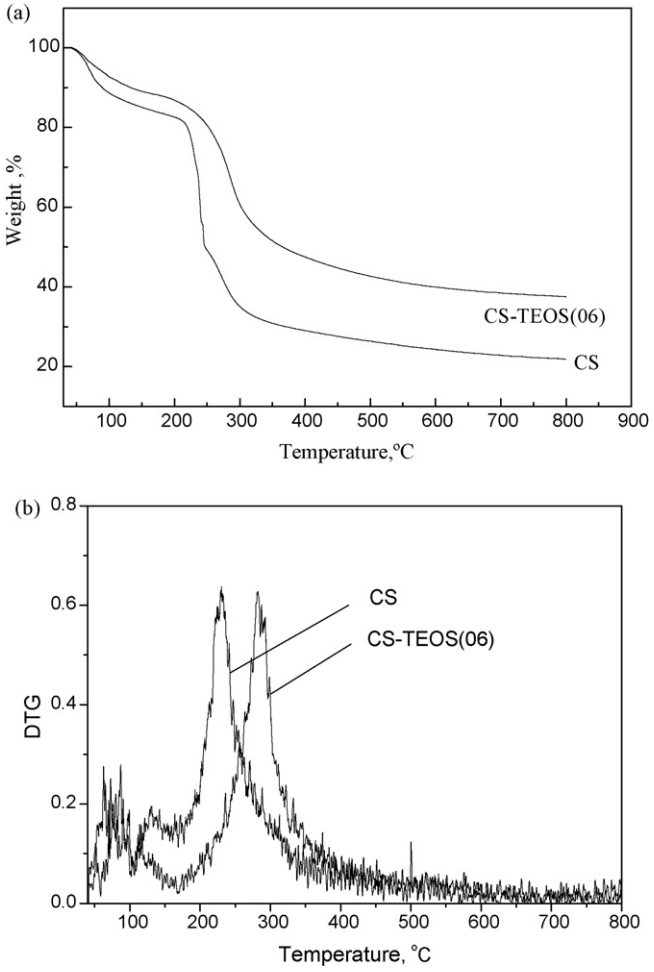

Fig. 4. TGA and DTG curves of chitosan pristine membrane and CS–TEOS (06) hybrid membrane.

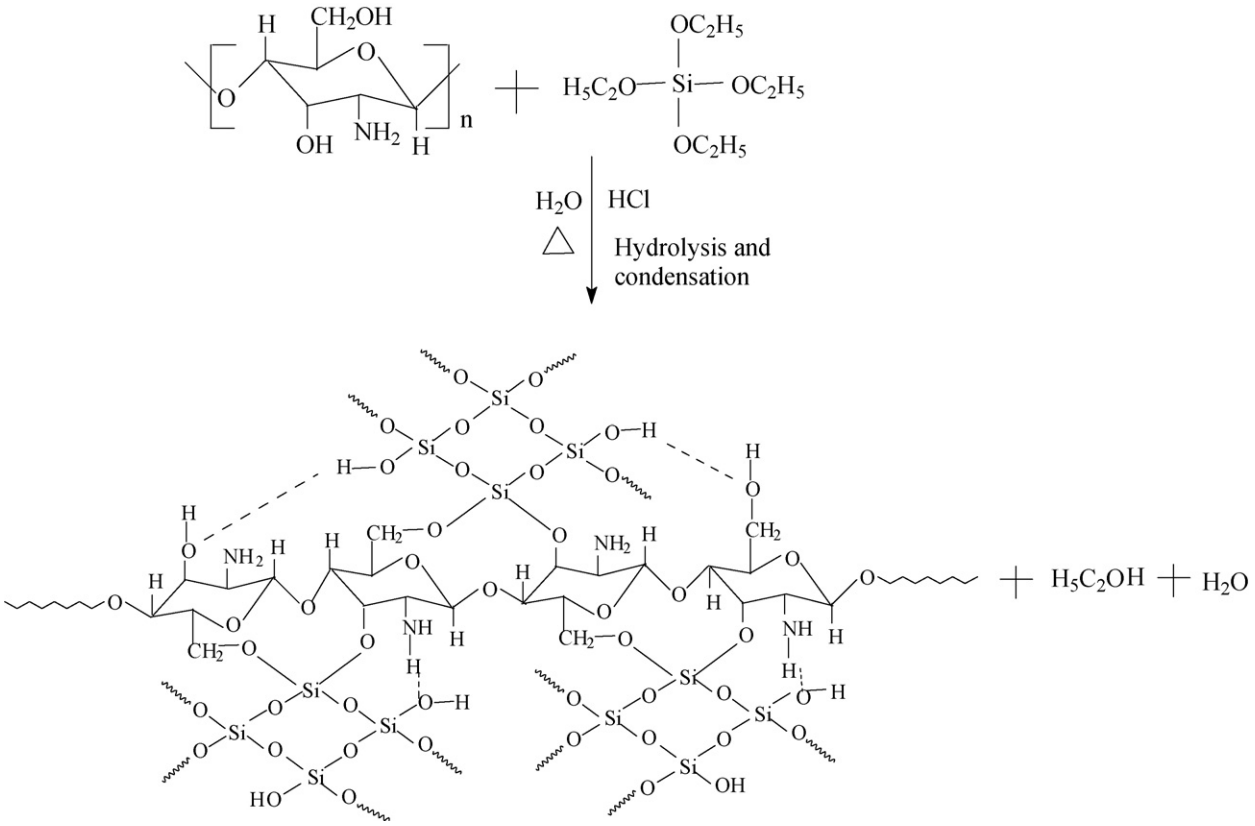

Fig. 5. Chemical structure and reaction routes of CS–TEOS hybrid membranes.

CS pristine membrane and CS–TEOS (10) membrane, respectively. It showed that the thermal stability of membranes was substantially improved after hybridization, which could be explained by the formation of Si—O—C bonds and hydrogen bonds between CS and generated SiO_2, as shown in Fig. 5.

Typical reaction temperatures in the esterification reactor can range approximately from 75 °C to 120 °C, therefore, the resulting CS–TEOS membranes should well meet the temperature requirements of esterification between lactic acid and ethanol.

3.1.4. Contact angle measurement

The contact angle for methylene iodide on the surface of CS pristine membrane and CS–TEOS membranes was measured and shown in Fig. 6. It could be seen that the contact angle of membranes increased with increasing the mass ratio of TEOS to CS, and were all higher than that of CS pristine membrane. These results implied that the hydrophilicity of CS–TEOS membranes was enhanced with increasing the mass ratio of TEOS to CS, which was attributed to the more hydrophilic groups liberated from the hydrolysis of TEOS.

3.2. Swelling and sorption properties of CS–TEOS membranes

Fig. 7 showed the effect of the mass ratio of TEOS to CS on the degree of swelling for CS–TEOS membranes. It could be seen that the degree of swelling of hybrid membranes were higher than CS pristine membrane, which attributed to the additional adsorption of generated SiO_2 inorganic particles to water and ethanol. Meanwhile, the degree of swelling decreased for hybrid membranes with increasing the mass ratio of TEOS to CS. This was because the sol–gel generated SiO_2 inorganic particles reacted as the joints among CS chain and the number of the joints increased with increasing the mass ratio of TEOS to CS, which would substantially restrict the polymer chain mobility.

Fig. 8 compared diffusion selectivity and solubility selectivity of CS–TEOS membranes with different mass ratio of TEOS to CS, the increasing amplitude of solubility selectivity was much smaller than that of diffusion selectivity, suggesting that diffusion selectivity played a dominant role in pervaporation process.

3.3. Pervaporation properties of CS–TEOS membranes

3.3.1. Effect of TEOS contents

As precursor of SiO_2 inorganic network, TEOS renders membrane resistant to swelling and restricts the mobility of the polymer

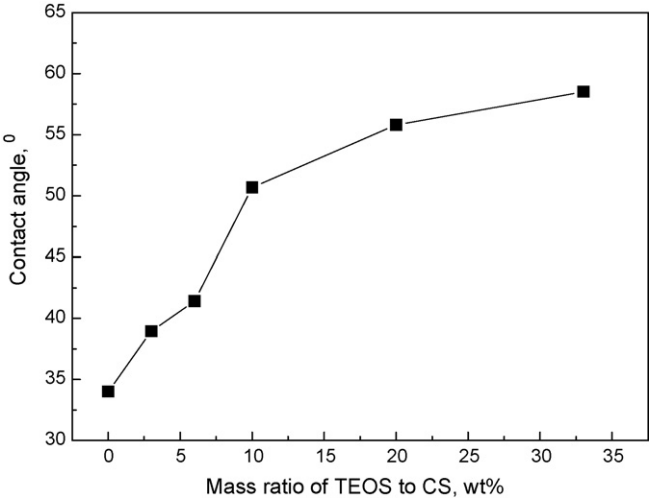

Fig. 6. Contact angle of CS–TEOS hybrid membranes with different mass ratio of TEOS to CS.

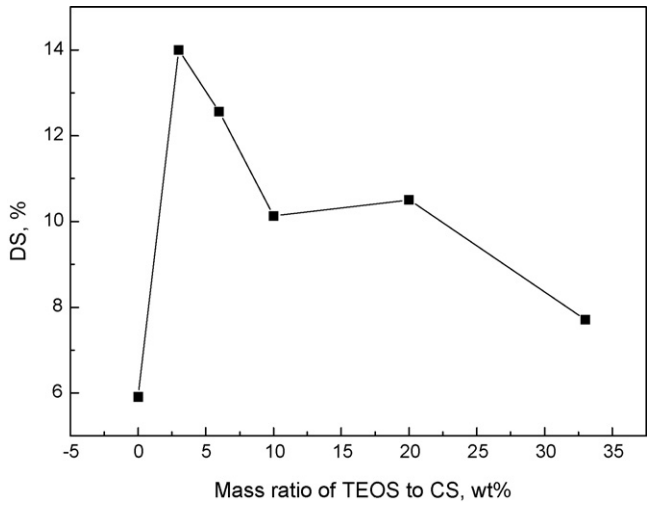

Fig. 7. Effect of mass ratio of TEOS to CS on the *DS* values of CS–TEOS hybrid membranes at 80 °C.

chains. Meanwhile, TEOS can adjust the hydrophilicity of the membrane material. In present study, the effect of mass ratio of TEOS to CS on pervaporation properties was studied and shown in Fig. 9. It demonstrated that both separation factor and permeation flux of CS–TEOS hybrid membranes were considerably higher than that of CS pristine membrane. The increase of separation factor was due to the increased hydrophilicity of CS–TEOS membranes, as testified by FT-IR and contact angle measurement. The increase of permeation flux was resulted from the decrease of crystallinity. Meanwhile, the permeation flux for CS–TEOS hybrid membranes decreased with increasing mass ratio of TEOS to CS. It could be explained by the decrease of degree of swelling (Fig. 7). Furthermore, as TEOS increasing, larger silica particles would form and thus elongated diffusion path. More energy would be needed when water and ethanol passed through the membrane, accordingly. The separation factor increased from 157 to 459 when the mass ratio of TEOS to CS increased from 3% to 6%, but the separation factor decreased to 299 when the mass ratio of TEOS to CS increased to 33%. The increase of separation factor was attributed to the increase of interaction between water molecules and the CS–TEOS membranes, which due to the more hydrophilic groups liberated from

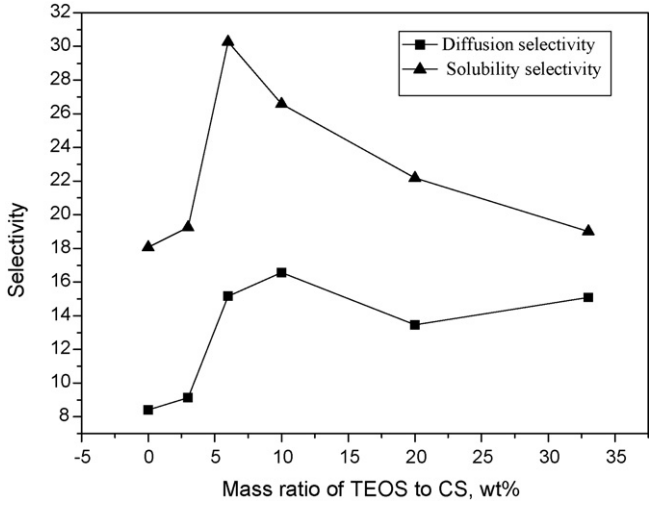

Fig. 8. Effect of mass ratio of TEOS to CS on the solubility selectivity and the diffusion selectivity of CS–TEOS hybrid membranes (10 wt.% water in aqueous ethanol solution, 80 °C).

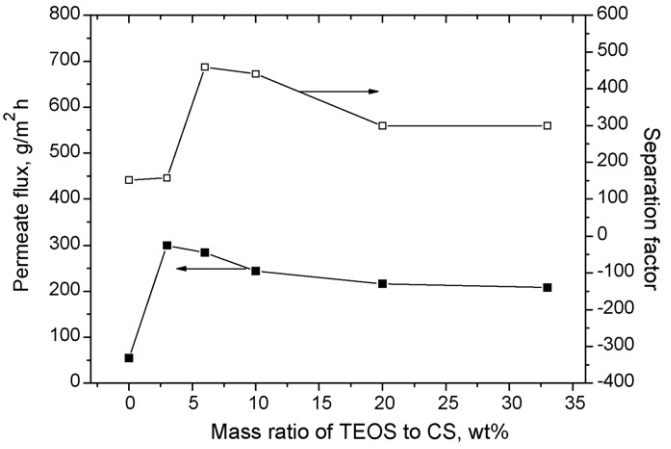

Fig. 9. Effect of mass ratio of TEOS to CS on the pervaporation properties (10 wt.% water in aqueous ethanol solution, 80 °C).

the hydrolysis of TEOS. But with more TEOS incorporated, formative SiO_2 particles were inclined to aggregate and appeared some non-ideal effects in membrane, leading to the separation factor decreased. As a result, CS–TEOS (06) membrane showed preferable separation properties in present study.

3.3.2. *Effect of operation temperature*

The effect of operating temperature ranging from 60 °C to 80 °C on the pervaporation properties of the CS–TEOS membrane was shown in Fig. 10. It could be observed that total flux increased notably, while the separation factor decreased with increasing temperature. It could be explained as follows: when operating temperature increased, vapor pressure of permeating components in the upstream side of membrane increased. Vapor pressure difference between the upstream and downstream side of the membrane enhanced the transport driving force. Moreover, increasing temperature brought about higher molecular diffusivity [42], therefore, the mass transport was faster and the total flux increased. In addition, as temperature increased, polymer chains became more flexible and accommodated larger available free volume of the polymer matrix for diffusion, which allowed both water and ethanol transfer across membrane easier and eventually the selectivity decreased.

3.3.3. *Effect of water content in the feed*

Fig. 11 illustrated the effect of water content in the feed varying from 2 wt.% to 15 wt.% on pervaporation properties of the CS–TEOS

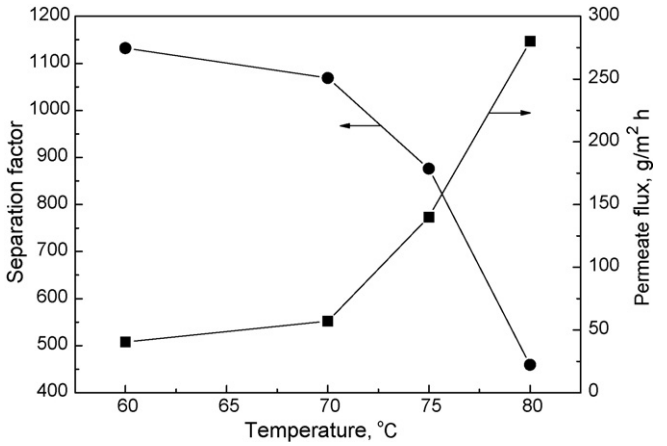

Fig. 10. Effect of operation temperature on the pervaporation flux and separation factor (CS–TEOS (06) membrane, 10 wt.% water in aqueous ethanol solution).

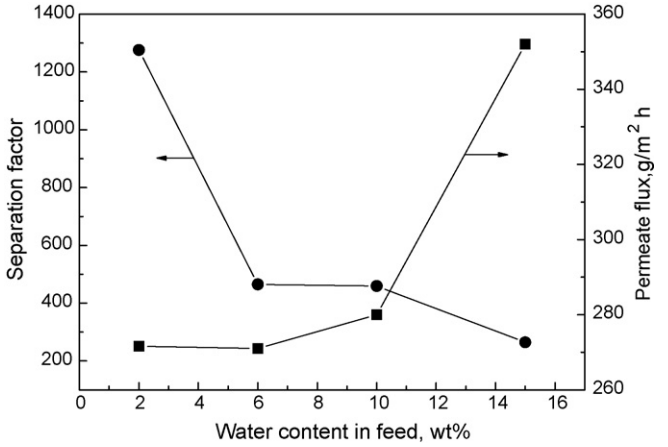

Fig. 11. Effect of water content in feed on the pervaporation flux and separation factor (CS–TEOS (06) membrane, 80 °C).

(06) membrane. With the increase of water content in the feed, the total flux increased from 271 g/(m^2 h) to 352 g/(m^2 h), while the separation factor decreased from 1380 to 268. It was attributed to that the *DS* value (shown in Fig. 12) of the CS–TEOS (06) membrane increased with increasing water content in the feed, leading to the reduction of mass transfer resistance and the acceleration of diffusion velocity for components in membrane. Meanwhile, the size of voids in membrane became larger and larger with increasing *DS* value, ethanol molecules won more chance to pass through these voids, which resulted in the decrease of separation factor.

The separation performance was governed comprehensively by both the solubility selectivity and the diffusion selectivity. As shown in Fig. 12, as the water content in feed mixture increased, the diffusion selectivity varied from 19.06 to 35.85 and the solubility selectivity varied from 13.85 to 30.60. These results indicated that the contribution of the diffusion selectivity to the separation factor variation was slightly larger than that of the solubility selectivity.

3.4. Pervaporation-assisted esterification process

As shown in Fig. 13, the yield of ethyl lactate was substantially enhanced due to the pervaporation process preferentially removed water from the reaction system and increased the reaction rate. Esterification without pervaporation achieved about 66 wt.% yield of ethyl lactate at a reaction temperature of 80 °C at 9 h,

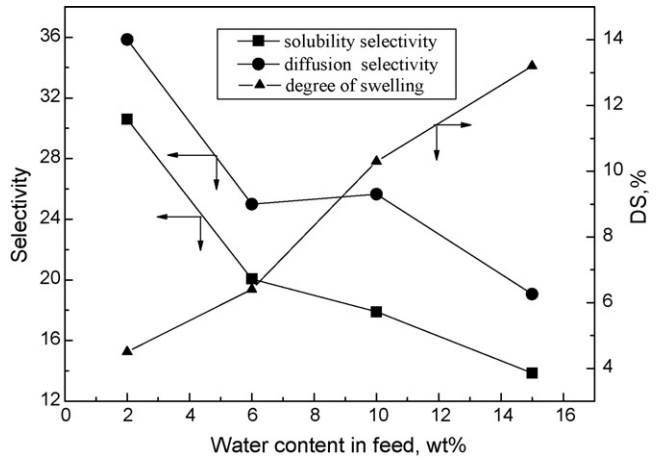

Fig. 12. Effect of the feed water content on the swelling, solubility and diffusion selectivity (CS–TEOS (06) membrane, 80 °C).

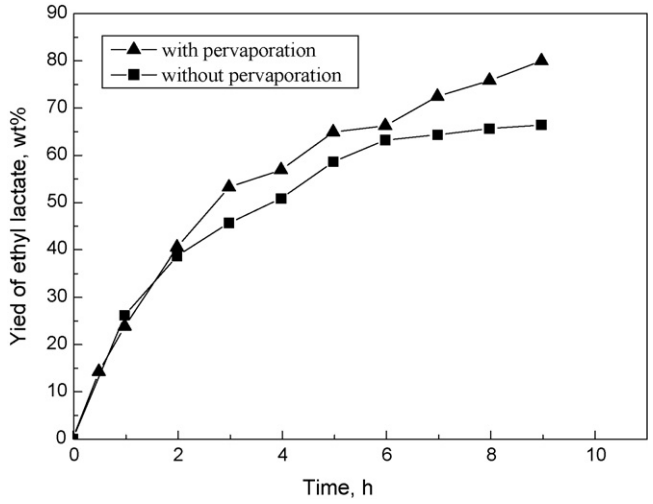

Fig. 13. Yield of ethyl lactate with and without pervaporation (T = 80 °C; $R_{E/L}$ = 3; $C_{catalyst}$ = 2.0 wt.% of lactic acid; CS–TEOS (06) membrane).

which increased to 80 wt.% when the esterification assisted by pervaporation.

The variation of water concentration in reaction mixture as a function of time for the esterification without and with pervaporation was listed in Fig. 14. For esterification process without pervaporation, water concentration in reaction mixture increased rapidly in the initial period because of the rapid reaction of esterification, and that was changed slightly almost after 3 h, because reaction rate of esterification became slowly gradually. When esterification assisted by pervaporation, water concentration in reaction mixture was lower than that for esterification without pervaporation and decreased after 3 h due to continuous water removal by pervaporation.

3.4.1. Effect of membrane recipe

Fig. 15 showed the effect of CS–TEOS membranes composition on yield of ethyl lactate in pervaporation-assisted esterification. The yield of ethyl lactate decreased when the mass ratio of TEOS to CS increased from 6 wt.% to 33 wt.%, which was in accordance with the tendency of pervaporation dehydration properties of membranes for ethanol/water mixture (as shown in Fig. 9). This phenomenon

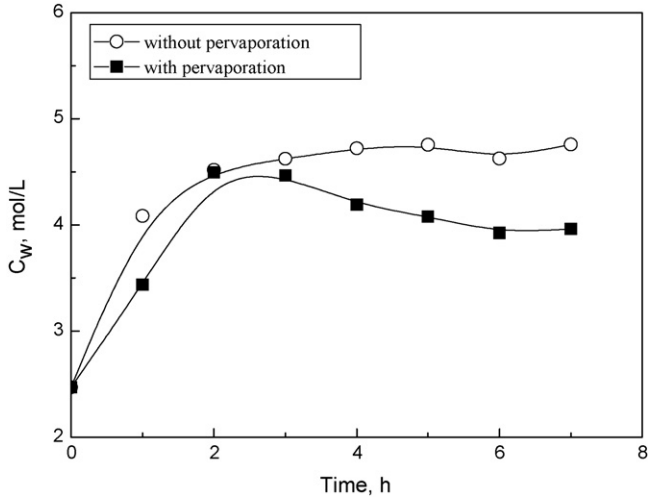

Fig. 14. Water concentration in reaction mixture for esterification both with and without pervaporation (T = 80 °C; $R_{E/L}$ = 3; $C_{catalyst}$ = 2.0 wt.% of lactic acid; CS–TEOS (06) membrane).

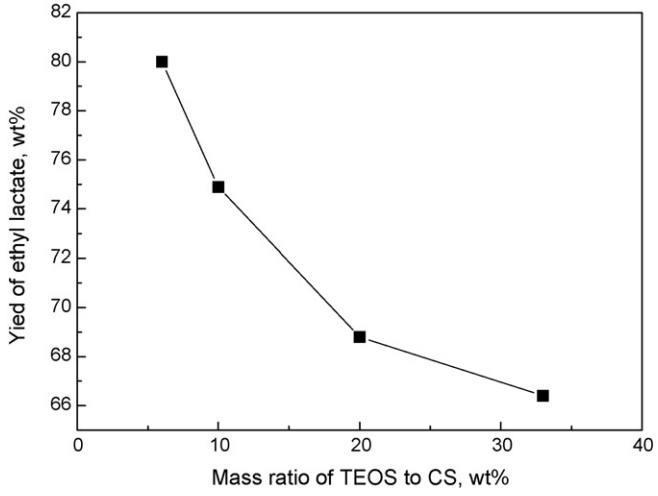

Fig. 15. Effect of pervaporation membrane composition on yield of ethyl lactate in pervaporation-assisted esterification (T = 80 °C; $R_{E/L}$ = 3; $C_{catalyst}$ = 2.0 wt.% of lactic acid; time = 9 h).

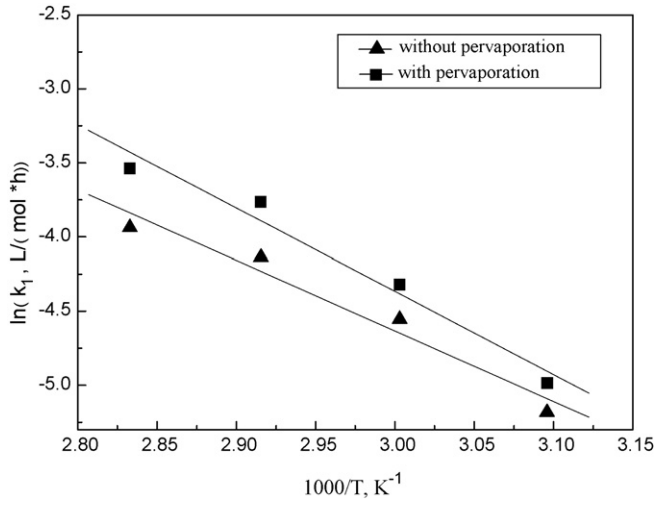

Fig. 16. Arrhenius curves of esterification with and without pervaporation ($R_{E/L}$ = 3; $C_{catalyst}$ = 2.0 wt.% of lactic acid; CS–TEOS (10) membrane).

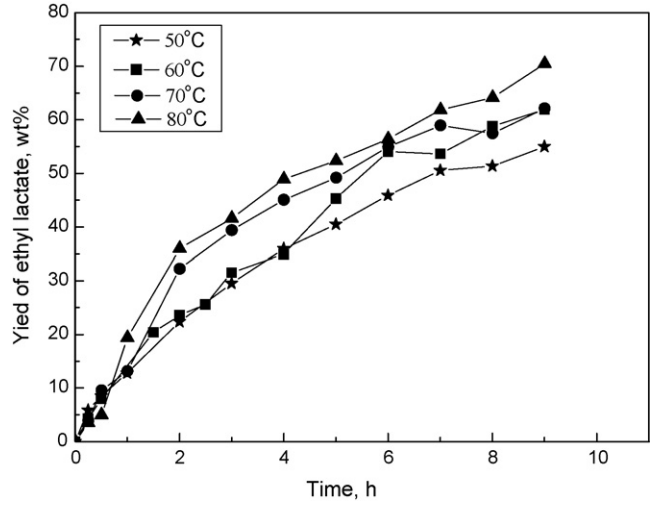

Fig. 17. Effect of reaction temperature on yield of ethyl lactate in pervaporation-assisted esterification ($R_{E/L}$ = 3; $C_{catalyst}$ = 2.0 wt.% of lactic acid; CS–TEOS (10) membrane).

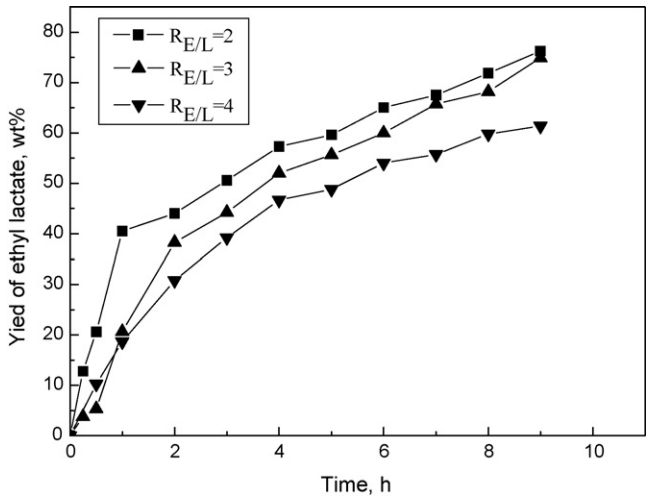

Fig. 18. Effect of $R_{E/L}$ on yield of ethyl lactate for pervaporation-assisted esterification (T = 80 °C; $C_{catalyst}$ = 2.0 wt.% of lactic acid; CS–TEOS (10) membrane).

indicated that the composition of CS–TEOS membranes affected the pervaporation properties, consequently, affected the yield of ethyl lactate in pervaporation-assisted esterification process.

3.4.2. Effect of reaction temperature

Temperature is a crucial influencing factor in esterification. Kinetic experiments were carried out in present study with a temperature range from 50 °C to 80 °C for esterification without and with pervaporation and the Arrhenius curves were shown in Fig. 16. It could be deduced that esterification of lactic acid and ethanol was an endothermic reaction. Accordingly, the yield of ethyl lactate increased with increasing reaction temperature in pervaporation-assisted esterification as shown in Fig. 17.

3.4.3. Effect of initial molar ratio ($R_{E/L}$) of ethanol to lactic acid

The initial molar ratio of ethanol to lactic acid ($R_{E/L}$) was ranged from 2 to 4 for pervaporation-assisted esterification reaction and its effect on the yield of ethyl lactate was shown in Fig. 18. It could be seen that the yield of ethyl lactate did not remarkably increase with the initial molar ratio of ethanol to lactic acid. This was due to the lactic acid used in present study was 88 wt.% lactic acid–water

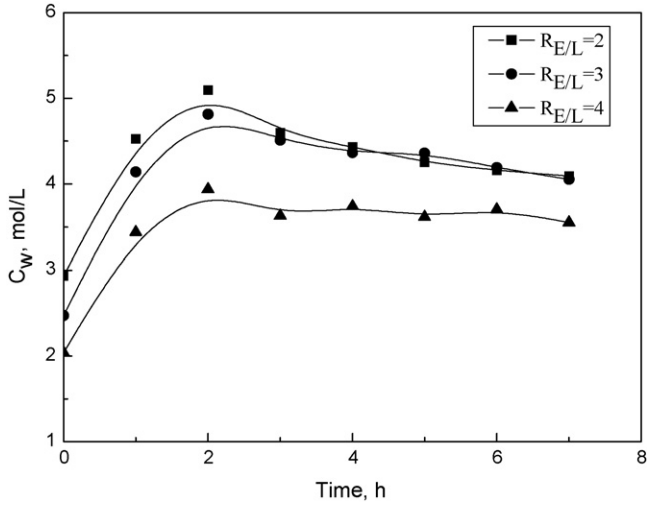

Fig. 19. Water concentration in reaction mixture for pervaporation-assisted esterification with different $R_{E/L}$ (T = 80 °C; $C_{catalyst}$ = 2.0 wt.% of lactic acid; CS–TEOS (10) membrane).

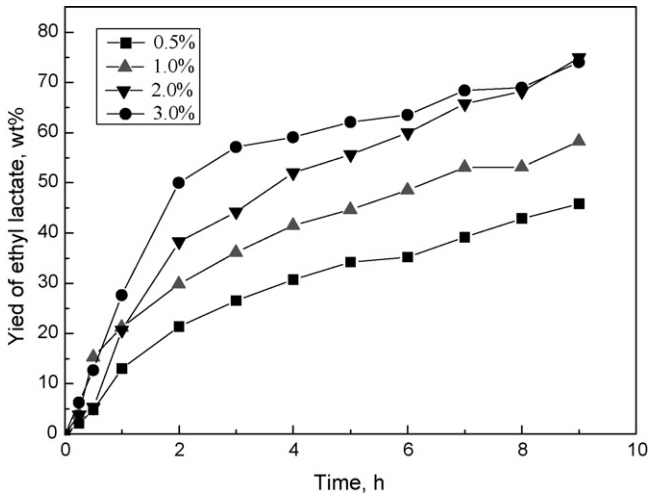

Fig. 20. Effect of catalyst concentration on yield of ethyl lactate in pervaporation-assisted esterification (T = 80 °C; $R_{E/L}$ = 3; CS–TEOS (10) membrane).

solution, amount of lactic acid–water solution used in esterification increased with decreasing $R_{E/L}$, which resulted in higher water concentration in reaction mixture (shown in Fig. 19) and rendered faster removal rate of water by pervaporation.

3.4.4. *Effect of catalyst loading*

The catalyst loading in this study was defined as the mass ratio of the catalyst to lactic acid and varied from 0.5 wt.% to 3.0 wt.%. It could be seen from Fig. 20 that the yield of ethyl lactate improved with the increase of catalyst loading as expected, because of the increasing catalyst active sites and decreasing of reaction activation energy which could obviously accelerate reaction rate.

4. Conclusion

The CS–TEOS organic–inorganic hybrid membranes for pervaporation-assisted esterification process were fabricated by in situ hydrolysis and condensation of TEOS within CS aqueous solution. The incorporation of TEOS enhanced the hydrophilicity and thermal stability and reduced the crystallinity of CS membrane.

The resulting CS–TEOS hybrid membrane showed a high selectivity towards water in the pervaporation separation of aqueous ethanol solution. The separation factor of 460 and permeation flux of 284 g/(m^2 h) were obtained for CS–TEOS (06) hybrid membrane with 10 wt.% water in feed at 80 °C.

The experimental results of pervaporation-assisted esterification revealed that incorporating pervaporation could effectively enhance the yield of ethyl lactate for esterification between ethanol and lactic acid. The effects of different operating parameters including composition of CS–TEOS membranes, reaction temperature, initial molar ratio of ethanol to lactic acid and catalyst loading on the process performance have been extensively investigated. Higher yield of ethyl lactate could be acquired with lower TEOS content in CS–TEOS membrane and initial molar ratio of ethanol to lactic acid, higher reaction temperature and catalyst loading.

Acknowledgements

The authors gratefully acknowledge the financial support from the National basic research program of China (2009CB623404), the Tianjin Science & Technology Research Program (06YFGPSH03400), the Programme of Introducing Talents of Discipline to Universities (No: B06006) and the Program for Changjiang Scholars and Innovative Research Team in University (PCSIRT).

References

[1] Y. Zhu, R.G. Minet, T.T. Tsotsis, A continuous pervaporation membrane reactor for the study of esterification reactions using a composite polymeric/ceramic membrane, Chem. Eng. Sci. 51 (1996) 4103–4113.
[2] X.S. Feng, R.Y.M. Huang, Studies of a membrane reactor: esterification facilitated by pervaporation, Chem. Eng. Sci. 51 (1996) 4673–4679.
[3] Q.L. Liu, Z.B. Zhang, H.F. Chen, Study on the coupling of esterification with pervaporation, J. Membr. Sci. 182 (2001) 173–181.
[4] X.H. Li, L.F. Wang, Kinetic model for an esterification process coupled by pervaporation, J. Membr. Sci. 186 (2001) 19–24.
[5] K. Tanaka, R. Yoshikawa, C. Ying, H. Kita, K. Okamoto, Application of zeolite membranes to esterification reactions, Catal. Today 67 (2001) 121–125.
[6] O. Iglesia, R. Mallada, M. Menendez, J. Coronas, Continuous zeolite membrane reactor for esterification of ethanol and acetic acid, Chem. Eng. J. 131 (2007) 35–39.
[7] D. Nemec, R. Gemert, Performing esterification reactions by combining heterogrneous catalysis and pervaporation in a batch process, Ind. Eng. Chem. Res. 44 (2005) 9718–9726.
[8] W.N. Lau, K.L. Yeung, R. Martin-Aranda, Knoevenage condensation reaction between benzaldehyde and ethyl acetoacetate in microreactor and membrane microreactor and membrane microreactor, Microporous Mesoporous Mater. 115 (2008) 156–163.
[9] X.F. Zhang, S.M. Lai, R. Martin-Aranda, K.L. Yeung, An investigation of knoevenagel condensation reaction in microreactors using new zeolite catalysts, Appl. Catal. A 261 (2004) 109–118.
[10] Y.S.S. Wan, J.L.H. Chau, A. Gavriilidis, K.L. Yeung, 1-Pentene epoxidation in catalytic microfabricated reactors, J. Catal. 223 (2004) 241–249.
[11] S.M. Lai, C.P. Ng, R. Martin-Aranda, K.L. Yeung, Knoevenagel condensation reaction in a zeolite membrane microreactor, Microporous Mesoporous Mater. 66 (2003) 239–252.
[12] S. Assabumrungrat, J. Phongpatthanapanich, P. Praserthdam, T. Tagawa, S. Goto, Theoretical study on the synthesis of methyl acetate from methanol and acetic acid in pervaporation membrane reactors: effect of continuous-flow modes, Chem. Eng. J. 95 (2003) 57–65.
[13] R. Krupiczka, Z. Koszorz, Activity-based model of the hybrid process of an esterification reaction coupled with pervaporation, Sep. Purif. Technol. 16 (1999) 55–59.
[14] D.J. Benedict, S.J. Parulekar, S.P. Tsai, Pervaporation-assisted esterification of lactic and succinic acids with downstream ester recovery, J. Membr. Sci. 281 (2006) 435–445.
[15] Q.L. Liu, H.F. Chen, Modeling of esterification of acetic acid with n-butanol in the presence of $Zr(SO4)_2{\cdot}4H_2O$ coupled pervaporation, J. Membr. Sci. 196 (2002) 171–178.
[16] C.Y. Tu, Y.L. Liu, K.R. Lee, Hydrophilic surface-grafted poly (tetrafluoroethylene) membranes using in pervaporation dehydration processes, J. Membr. Sci. 274 (2006) 47–55.
[17] M.Y. Kariduraganavar, A.A. Kittur, S.S. Kulkarni, Development of novel pervaporation membranes for the separation of water–isopropanol mixtures using sodium alginate and NaY zeolite, J. Membr. Sci. 238 (2004) 165–175.
[18] T. Uragami, S. Yanagisawa, T. Miyata, Water/ethanol selectivity of new organic–inorganic hybrid membranes fabricated from poly(vinyl alcohol) and an oligosilane, Macromol. Chem. Phys. 208 (2007) 756–764.
[19] Y.L. Liu, Y.H. Su, K.R. Lee, J.Y. Lai, Crosslinked organic–inorganic hybrid chitosan membranes for pervaporation dehydration of isopropanol–water mixtures with a long-term stability, J. Membr. Sci. 251 (2005) 233–238.
[20] Y. Yang, J.W. Qian, L.J. Xuan, A.F. An, L. Zhang, C.J. Gao, Preparation and pervaporation of a palygorskite/polyacrylamide inorganic–organic hybrid membrane for separating m-/p-xylene isomers, Desalination 193 (2006) 193–201.
[21] H. Cong, M. Radosz, B.F. Towler, Y. Shen, Polymer–inorganic nanocoposite membranes for gas separation, Sep. Purif. Technol. 55 (2007) 281–291.
[22] P.M. Budd, N.M.P.S. Ricardo, J.J. Jafar, B. Stephenson, R. Hughes, Zeolite/polyelectrolyte multilayer pervaporation membranes for enhanced reaction yield, Ind. Eng. Chem. Res. 43 (2004) 1863–1867.
[23] S.G. Adoor, L.S. Manjeshwar, S.D. Bhat, T.M. Aminabhavi, Aluminum-rich zeolite beta incorporated sodium alginate mixed matrix membranes for pervaporation dehydration and esterification of ethanol and acetic acid, J. Membr. Sci. 31 (2008) 233–246.
[24] J. Li, L.H. Zhu, Y.H. Wu, Y. Harima, A.Q. Zhang, H.Q. Tang, Hybrid composites of conductive polyaniline and nanocrystalline titanium oxide prepared via self-assembling and graft polymerization, Polymer 47 (2006) 7361–7367.
[25] B. Hojjati, R. Sui, P.A. Charpentier, Synthesis of TiO_2/PAA nanocomposite by RAFT polymerization, Polymer 48 (2007) 5850–5858.
[26] P. MaĖki-Arvelaa, T. Salmia, M. Sundellb, K. Ekmanb, R. Peltonenb, J. Lehtonen, Comparison of polyvinylbenzene and polyolen supported sulphonic acid catalysts in the esterification of acetic acid, Appl. Catal. A: Gen. 184 (1999) 25–32.
[27] J.J. Jafar, P.M. Budda, R. Hughes, Enhancement of esterification reaction yield using zeolite A vapour permeation membrane, J. Membr. Sci. 199 (2002) 117–123.
[28] A. Izci, F. Bodur, Liquid-phase esterification of acetic acid with isobutanol catalyzed by ion-exchange resins, React. Funct. Polym. 67 (2007) 1458–1464.
[29] S.R. Kirumakki, N. Nagaraju, S. Narayanan, A comparative esterification of benzyl alcohol with acetic acid over zeolites Hβ, HY and HZSM5, Appl. Catal. A: Gen. 273 (2004) 1–9.

[30] F. Omota, A.C. Dimian, A. Bliek, Fatty acid esterification by reactive distillation. Part 2. Kinetics-based design for sulphated zirconia catalysts, Chem. Eng. Sci. 58 (2003) 3175–3185.
[31] T.A. Peters, N.E. Benes, A. Holmen, J.T.F. Keurentjes, Comparison of commercial solid acid catalysts for the esterification of acetic acid with butanol, Appl. Catal. A: Gen. 297 (2006) 182–188.
[32] Y.H. Liu, Q.S. Liu, Z.H. Zhang, Amberlyst-15 as a new and reusable catalyst for regioselective ring-opening reactions of epoxides to β-alkoxy alcohols, J. Mol. Catal. A: Chem. 296 (2008) 42–46.
[33] T.A. Peters, N.E. Benes, A. Holmen, J.T.F. Keurentjes, Comparison of commercial solid acid catalysts for the esterification of acetic acid with butanol, Appl. Catal. A 297 (2006) 182–188.
[34] G.D. Yadav, M.B. Thathagar, Esterification of maleic acid with ethanol over cation-exchange resin catalysts, React. Funct. Polym. 52 (2002) 99–110.
[35] M.T. Sanz, J. Gmehling, Esterification of acetic acid with isopropanol coupled with pervaporation. Part I. Kinetics and pervaporation studies, Chem. Eng. J. 123 (2006) 1–8.
[36] S. Matsui, D.R. Paul, Pervaporation separation of aromatic/aliphatic hydrocarbons by crosslinked poly(methyl acrylate-co-acrylic acid) membranes, J. Membr. Sci. 195 (2002) 229–245.
[37] H.L. Sun, L.Y. Lu, X. Chen, Z.Y. Jiang, Pervaporation dehydration of aqueous ethanol solution using H-ZSM-5 filled chitosan membranes, Sep. Purif. Technol. 58 (2008) 429–436.
[38] G. Dhanuja, B. Smitha, S. Sridhar, Pervaporation of isopropanol/water mixtures through polyion complex membranes, Sep. Purif. Technol. 44 (2005) 130–138.
[39] L.Y. Lim, L.S.C. Wan, Heat treatment of chitosan films, Drug Dev. Ind. Pharm. 21 (1995) 839–846.
[40] K. Ogawa, Effect of heating an aqueous suspension of chitosan on the crystalinity and polymorphs, Agric. Biol. Chem. 55 (1991) 2375–2379.
[41] D. Britto, S.P. Campana-Filho, A kinetic study on the thermal degradation of N,N,N-trimethyl chitosan, Polym. Degrad. Stab. 84 (2004) 353–361.
[42] A. Svang-Ariyaskul, R.Y.M. Huang, P.L. Douglas, R. Pal, X. Feng, P. Chen, L. Liu, Blended chitosan and polyvinyl alcohol membranes for the pervaporation dehydration of isopropanol, J. Membr. Sci. 280 (2006) 815–823.